

LAPTH-820/00
Edinburgh 2000/28
December 2000

Beyond leading order effects in photon pair production at the Tevatron

T. Binoth^{a,b}, J. Ph. Guillet^a, E. Pilon^a and M. Werlen^a

^a *Laboratoire d'Annecy-Le-Vieux de Physique Théorique¹ LAPTH,
Chemin de Bellevue, B.P. 110, F-74941 Annecy-le-Vieux, France*

^b *Department of Physics and Astronomy, University of Edinburgh,
Edinburgh EH9 3JZ, Scotland*

Abstract

We discuss effects induced by beyond leading order contributions to photon pair production. We point out that next to leading order contributions to the fragmentation component of the signal lead to a change in the shape of distributions. This is already mildly visible in present Tevatron data though stringent isolation criteria tend to suppress the fragmentation component considerably. We expect the effect to be experimentally confirmed in future data samples with higher statistics which would serve as a precision test for QCD.

¹UMR 5108 du CNRS, associée à l'Université de Savoie.

1 Introduction

The production of prompt photon pairs with large invariant mass is the object of continuing experimental studies ranging from fixed target [1, 2, 3], to colliders energies [4, 5, 6], especially by the CDF and D0 experiments at the Tevatron. The word “prompt” means that these photons do not come from the decays of hadrons such as π^0 , η , etc. at large transverse momentum. Prompt photons may be produced according to two possible mechanisms: either they take part directly to the hard subprocess (direct mechanism), or they result from the fragmentation of large transverse momentum partons (fragmentation mechanism). For a general discussion of the production mechanisms of prompt photon pairs, see Ref. [7]. Besides offering an interesting probe of the short distance QCD dynamics, di-photon hadroproduction is the irreducible background for the search of a neutral Higgs boson in the channel $H \rightarrow \gamma\gamma$ in the mass range 90 - 140 GeV at the LHC, which provides a strong motivation for its extensive study.

Collider experiments at the Tevatron and the forthcoming LHC do not perform *inclusive* photon measurements. Indeed, the inclusive production rates of $\gamma\pi^0$ and $\pi^0\pi^0$ pairs with large invariant mass are orders of magnitude larger than the one of prompt photon pairs, to which they provide the background. Thus the experimental selection of prompt photons requires the use of isolation cuts. The isolation criterion used by the Tevatron experiments CDF [5] and D0 [6] is schematically the following. A photon is said to be isolated if, in a cone in rapidity and azimuthal angle about the photon direction, the amount of deposited hadronic transverse energy E_T^{had} is smaller than some value $E_{T\max}$ fixed by the experiment:

$$E_T^{had} \leq E_{T\max} \quad \text{inside} \quad (y - y_\gamma)^2 + (\phi - \phi_\gamma)^2 \leq R^2 \quad (1)$$

The actual experimental criteria, which are defined at the detector level, are much more complicated than the simple one given by Eqn. (1), see [5, 6]. They cannot be implemented in a partonic calculation. The schematical criterion of Eqn. (1) is a modelization of their effects at the parton level. The topic of isolation of photons based on the above criterion is extensively discussed in the literature [8, 9, 10, 11, 12, 13]. Besides the rejection of the background of secondary photons, the isolation cut also reduces the prompt photons from fragmentation. The stringent isolation requirements used by CDF and D0 suppress the fragmentation component quite a lot; therefore, the effects of the fragmentation component are generally neglected beyond their lowest order in perturbation theory. Yet they can affect various observables in a sizeable way. For example, in the case of single photon production, it yields a significant increase in the transverse momentum distribution in the lower range of the p_T spectrum [11, 12, 13].

In a recent work, we presented a full next to leading order (NLO) study of di-photon hadroproduction based on a computer code of partonic event generator type, *DIPHOX* [7]. In this short article, relying on this general study, we illustrate the impact of beyond leading order contributions, especially to the fragmentation component, in di-photon production at the Tevatron.

2 Impact of higher order corrections on di-photon spectra

Higher order QCD contributions to a given observable lead to a refinement of theoretical predictions in several aspects. If already the Born level contains the strong coupling α_s , higher orders stabilize dependencies on arbitrary scales stemming from the truncation of the perturbative series. In the hadronic production of direct photon pairs this is not the case though it is in general true for the fragmentation parts. Furthermore, the inclusion of the NLO contributions allow for new initial states. The additional production channels are typically the reason for large K factors. But higher order contributions also modify final state observables, as extra particles in the final state generate kinematical configurations which are forbidden at leading order and lead to sizeable ef-

fects², especially if new collinear situations in the final states are possible. Such effects can be seen in observables sensitive to kinematical configurations where the photons are emitted in rather close directions to each other. Indeed, such configurations contribute only beyond leading order (at lowest order, transverse momentum conservation forces the photons to be back to back in the transverse plane). Moreover, the contribution of such configurations coming from the fragmentation mechanism is enhanced, as will be discussed below.

A typical representative of this family of observables is the distribution $d\sigma/dq_T$ of transverse momentum of di-photons ($q_T = ||\vec{p}_T(\gamma_1) + \vec{p}_T(\gamma_2)||$). Fig. 1 shows the comparison between the D0 preliminary data and our theoretical computation taking into account the kinematic and isolation cuts of the D0 Tevatron experiment. D0 requires $|y(\gamma_{1,2})| < 1.0$ for the photon rapidities, and the lower experimental p_T cuts are

$$p_T(\gamma_1) \geq 14 \text{ GeV}, \quad p_T(\gamma_2) \geq 13 \text{ GeV} \quad (2)$$

which roughly correspond to effective cuts at respectively

$$p_{T\min}(\gamma_1) = 14.90 \text{ GeV}, \quad p_{T\min}(\gamma_2) = 13.85 \text{ GeV} \quad (3)$$

in a partonic calculation³. Furthermore, a lower cut in the two-photon acollinearity is required:

$$(y(\gamma_1) - y(\gamma_2))^2 + \phi_{\gamma\gamma}^2 \geq R_{\min}^2 \quad (4)$$

where $\phi_{\gamma\gamma}$ is the photon-photon azimuthal angle and $R_{\min} = 0.3$. The isolation criterion is modeled according to Eqn. (1) with $E_{T\max} = 2 \text{ GeV}$, $R = 0.4$.

One can see a shoulder at about $q_T \sim 35 \text{ GeV}$ in the distribution measured experimentally. At first glance, one may question its significance, given the limited statistics of the Run I data and the systematic uncertainties which affect these preliminary data. However a corresponding shoulder appears in the theoretical calculation performed with the same binning as the data too. A careful study reveals that this shoulder is not a mere statistical fluctuation of the partonic Monte-Carlo generator, nor a binning artefact, but it is a physical effect.

In order to see this, we split the two-photon phase space into regions, according to the photon-photon azimuthal angle $\phi_{\gamma\gamma}$:

$$\text{Region I: } 0 \leq \phi_{\gamma\gamma} < \frac{\pi}{2}; \quad \text{Region II: } \frac{\pi}{2} \leq \phi_{\gamma\gamma} \leq \pi. \quad (5)$$

Since at leading order, the two body kinematics forces the photons to be back to back in the transverse momentum plane ($\phi_{\gamma\gamma} = \pi$), the leading order contributions to $d\sigma/dq_T$ come entirely from region II, and vanish in region I. With respect to the above artificial slicing (5), a “new channel” opens at NLO - and beyond - which populates region I. However, as $q_T = ||\vec{p}_T(\gamma_1) + \vec{p}_T(\gamma_2)||$, the asymmetric cuts on the p_T ’s of the photons imply that the contribution to $d\sigma/dq_T$ from region I vanishes for $q_T \leq q_{T\min}$ with $q_{T\min} = (p_{T\min}^2(\gamma_1) + p_{T\min}^2(\gamma_2))^{1/2}$, so that this “new channel” opens only above $q_{T\min} \simeq 20.34 \text{ GeV}$. It is instructive to examine separately the direct, and the fragmentation components⁴ above this threshold.

²Higher order corrections can also reveal new infrared sensitive issues, in particular *inside* the physical spectrum, as it is the case for the q_T distribution at $q_T = E_{T\max}$ [7].

³The experimental cuts at measured values 14 and 13 GeV respectively in the D0 data are not corrected for the electromagnetic calorimeter absolute energy scale. See [7] for more details.

⁴We call *direct* the mechanism by which both photons take part to the hard subprocess, *one fragmentation* the one by which one photon takes part to the hard subprocess whereas the other comes from fragmentation, and *two fragmentation* the one by which both photons come from fragmentation. We call *fragmentation* the sum of these last two components. Actually, the severe isolation cut used by D0 suppresses the *two fragmentation* component down to a completely negligible level. Consequently, we will ignore it in the present discussion.

The direct component is displayed on Fig. 2(a). As q_T increases above $q_{T\min}$, the size of the opening slice of available phase space belonging to region I becomes comparable with the one of region II. The direct component, which starts at NLO for $q_T \geq q_{T\min}$, is by definition free of any final state collinear singularity. It thus involves only smooth variations with $(y(\gamma_1) - y(\gamma_2))$ and $\phi_{\gamma\gamma}$. Therefore, after a transition regime extending up to $q_T \leq 35 - 40$ GeV, the magnitudes of the contributions from regions I and II become comparable. Moreover the R_{\min} dependence, which comes from region I, is weak, $\mathcal{O}(R_{\min}^2)$ at small R_{\min} . In summary the approximate doubling of available phase space due to the opening of region I above $q_{T\min}$ roughly amounts to a doubling of the direct component.

On the contrary, the fragmentation component is collinearly enhanced when the two photons come close to each other. Indeed, without the cut (4), contributions such as the one pictured in Fig. 3 would make the fragmentation component logarithmically divergent for all q_T larger than $q_{T\lim} = p_{T\min}(\gamma_1) + p_{T\min}(\gamma_2)$ with $q_{T\lim} \simeq 28.75$ GeV. This divergence would be produced when the photon considered as “direct” would become collinear to the one from fragmentation⁵. The acollinearity cut (4) forbids this configuration; yet a collinear enhancement survives in region I as a memory of this regime. As the slice of available phase space in region I opens, the fragmentation contribution from this region rises initially faster than the contribution from region II decreases above $q_{T\min}$. This generates a peak in the fragmentation component about $q_T \sim 30-35$ GeV, until the contribution from region I decreases too. As a reflect of the collinear enhancement, the smaller the value of R_{\min} , the higher the peak. For $q_{T\min}$ above 25-30 GeV, the fragmentation term comes mostly from region I, contrarily to the direct case. This is illustrated on Fig. 2 which compares the case $R_{\min} = 0.3$ experimentally used and what would happen for $R_{\min} = 0.01$, an artifical value chosen on purpose to emphasize this effect.

Due to the fact that the fragmentation component is severely suppressed by the isolation cut (1) with respect to the direct one, and that the value $R_{\min} = 0.3$ experimentally used leads to a rather moderate enhancement of this fragmentation component, the effect of the latter is limited to a 10% modulation effect in the total (= direct + fragmentation) distribution, so that the shoulder is mainly due to the direct component. This can be seen in Fig. 4 showing the ratio total/direct. However, the effect would be more spectacular with lower values of R_{\min} . For illustrative purpose, Fig. 4 also shows what would be the situation with the value $R_{\min} = 0.01$.

The collinear enhancement in the fragmentation component affects also the distribution $d\sigma/d\phi_{\gamma\gamma}$ of azimuthal angle between the two photons in a pair, in the lower range of the $\phi_{\gamma\gamma}$ spectrum, cf. Fig. 5. The contribution of the direct component decreases monotonically while remaining finite when $\phi_{\gamma\gamma} < \pi$ decreases towards 0. Instead, the fragmentation contribution to this observable would diverge logarithmically at $\phi_{\gamma\gamma} = 0$ without the acollinearity cut (4), as can be inferred from Fig. 6. The fragmentation contribution “feels” this collinear divergence by rising again when $\phi_{\gamma\gamma}$ decreases below ~ 1 towards R_{\min} . This divergence is forbidden by the constraint (4). The latter produces a turnover when $\phi_{\gamma\gamma} \leq R_{\min}$, which can be seen on the right plot on the right of Fig. 6 in the lower range of the spectrum.

One may wonder about the significance of these effects compared with the theoretical scale uncertainties associated with the arbitrariness of the renormalization and factorization scales used

⁵From a theoretical point of view, the subtraction of the corresponding double collinear divergence for the {partonic emitter + two photons} system in the partonic calculation would require a new type of fragmentation functions of partons into “twin collinear photons”, extending the procedure corresponding to the case of fragmentation into a single photon. Such collinear photons would actually be detected as single photon events. Most probaby they would contribute to the single photon production rate at a negligeable level, at least in the Tevatron energy range, due to a relative suppression factor $\propto \mathcal{O}(\alpha_{em})$ with respect to the typical single photon production rate. In practice, the experimental cuts on the acollinearity $(y(\gamma_1) - y(\gamma_2))^2 + \phi_{\gamma\gamma}^2$ of the two photons, or on the invariant mass of the pair, prevent from having to consider this regime.

in the partonic calculation⁶. Concerning the q_T distribution, the direct contribution to the tail of the distribution above $q_{T\ min}$ starts at NLO (the Born contribution to the direct component is concentrated at $q_T = 0$ by transverse momentum conservation). As for the $\phi_{\gamma\gamma}$ distribution, both the direct and fragmentation contributions to the tail of the distribution away from $\phi_{\gamma\gamma} = \pi$ start at NLO too (the respective Born terms being concentrated at $\phi_{\gamma\gamma} = \pi$). For each of these two observables, NLO is the *effective* lowest order. Consequently, it is fair to say that these uncertainties are rather large. However scale uncertainties act roughly as an overall effect: they do not generate local distortions comparable to the pattern of effects studied above. We insist that the latter are *physical* effects, which could in principle be unambiguously observed among data with higher statistics and an improved understanding of systematics, as it may hopefully be the case in the forthcoming Run II of the Tevatron.

3 Conclusions and perspectives.

In this note we have emphasized NLO effects, coming in particular from the fragmentation contribution to di-photon production. We have pointed out that a new collinear sensitive situation arises in the fragmentation part at next to leading order, namely when the two photons become more and more close to each other. This leads to an enhancement of the respective signal. Stringent isolation criteria reduce the fragmentation contribution considerably and acollinearity cuts between the two photons forbid collinear photons in the experimental situation. Consequently, these next to leading order effects from fragmentation are not very significant in the present data. However we have shown that the account of these contributions is required for an accurate description of the shapes of di-photon observables. They thus may become relevant for a precise understanding of the high statistic data to be collected during the forthcoming Run II at the Tevatron.

Acknowledgments. This work was supported in part by the EU Fourth Training Programme “Training and Mobility of Researchers”, Network “Quantum Chromodynamics and the Deep Structure of Elementary Particles”, contract FMRX-CT98-0194 (DG 12 - MIHT). LAPTH is a Unité Mixte de Recherche (UMR 5108) du CNRS associée à l’Université de Savoie.

References

- [1] WA70 Collaboration, E. Bonvin *et al.*, Z. Phys. **C41** (1989) 591.
- [2] WA70 Collaboration, E. Bonvin *et al.*, Phys. Lett. **236B** (1990) 523.
- [3] M. Begel, private communication (E706 collaboration).
- [4] UA2 Collaboration. J. Alitti *et al.*, Phys. Lett. **288B** (1992) 386.
- [5] CDF Collaboration, F. Abe *et al.*, Phys. Rev. Lett. **70** (1993) 2232.
- [6] Wei Chen, PhD Thesis (Univ. New-York at Stony Brook), Dec. 1997, unpublished;
D0 Collaboration (P. Hanlet for the collaboration), Nucl. Phys. Proc. Suppl. **64** (1998) 78.
All the numbers used in this article are taken from tables in Wei Chen’s PhD Thesis.
- [7] T. Binoth, J.P. Guillet, E. Pilon and M. Werlen, Eur. Phys. J. **C16** (2000) 311.
- [8] H. Baer, J. Ohnemus and J.F. Owens, Phys. Rev. **D42** (1990) 61.

⁶For definiteness, we used the common scale $M = M_F = \mu = (p_T(\gamma_1) + p_T(\gamma_2))/4$ for the initial state factorization, final state fragmentation, and renormalization scales.

- [9] P. Aurenche, R. Baier and M. Fontannaz, Phys. Rev. **D42** (1990) 1440.
- [10] E.L. Berger and J. Qiu, Phys. Rev. **D44** (1991) 2002.
- [11] L.E. Gordon and W. Vogelsang, Phys. Rev. **D50** (1994) 1901.
- [12] W. Vogelsang and A. Vogt, Nucl.Phys. **B453** (1995) 334.
- [13] S. Catani, M. Fontannaz, J.P. Guillet and E. Pilon, work in preparation.

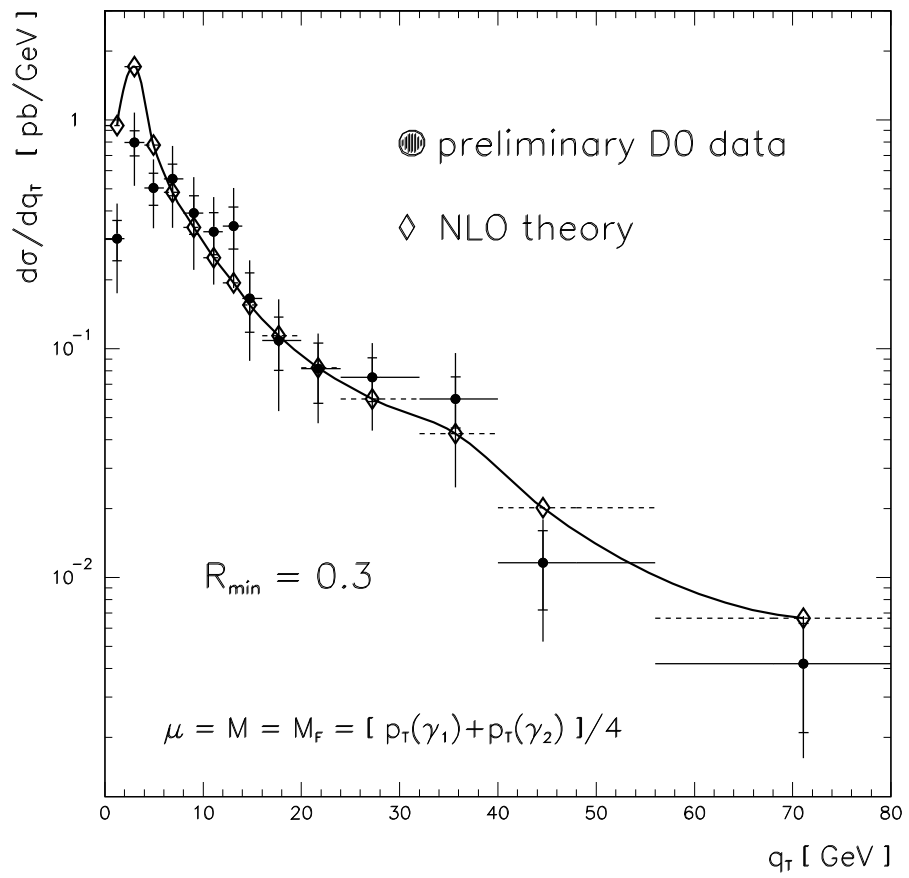


Figure 1: q_T distribution of photon pairs. Black dots: D0 data [6]; white diamonds: average values of the NLO calculation (DIPHOX code) in the corresponding experimental bins. The curve is a spline interpolation between the theoretical average.

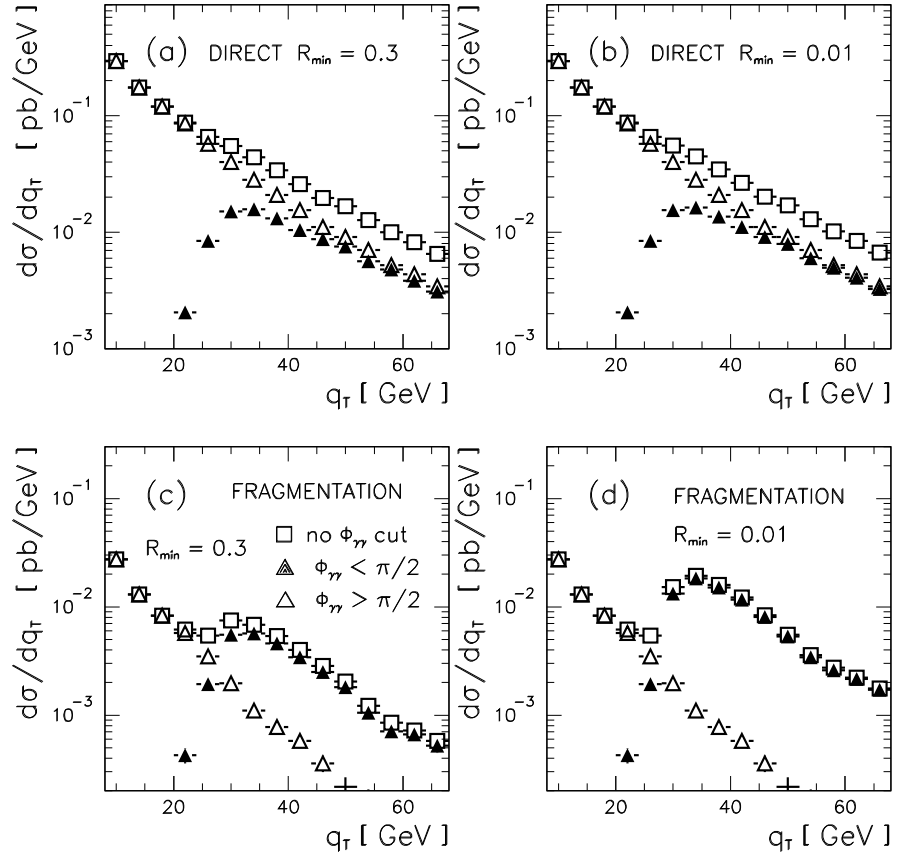


Figure 2: Origin of the q_T shoulder in the theoretical calculation. Plot (a) shows the direct component (open squares) split into the phase space regions $\phi_{\gamma\gamma} < \pi/2$ (full triangles) and $\phi_{\gamma\gamma} > \pi/2$ (open triangles) for the experimentally used value $R_{min} = 0.3$. Plot (b) is the same as (a) but for $R_{min} = 0.01$ to show the sensitivity of the effect to this collinear cut. Plots (c) and (d) show the corresponding histograms for the fragmentation component where the enhancement due to photon collinearity is clearly visible.

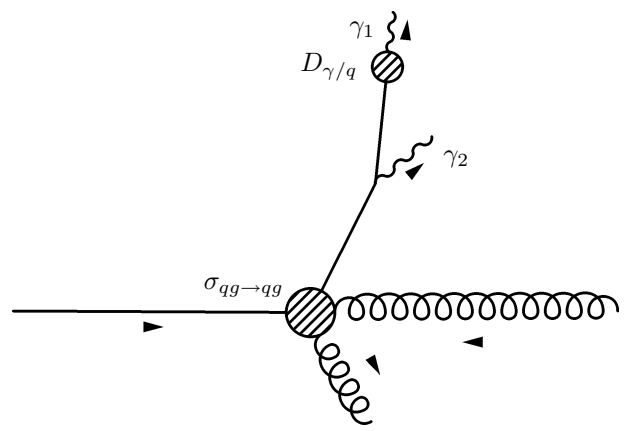


Figure 3: Kinematical configuration for which the fragmentation contribution is collinearly enhanced when the two photons become close to each other.

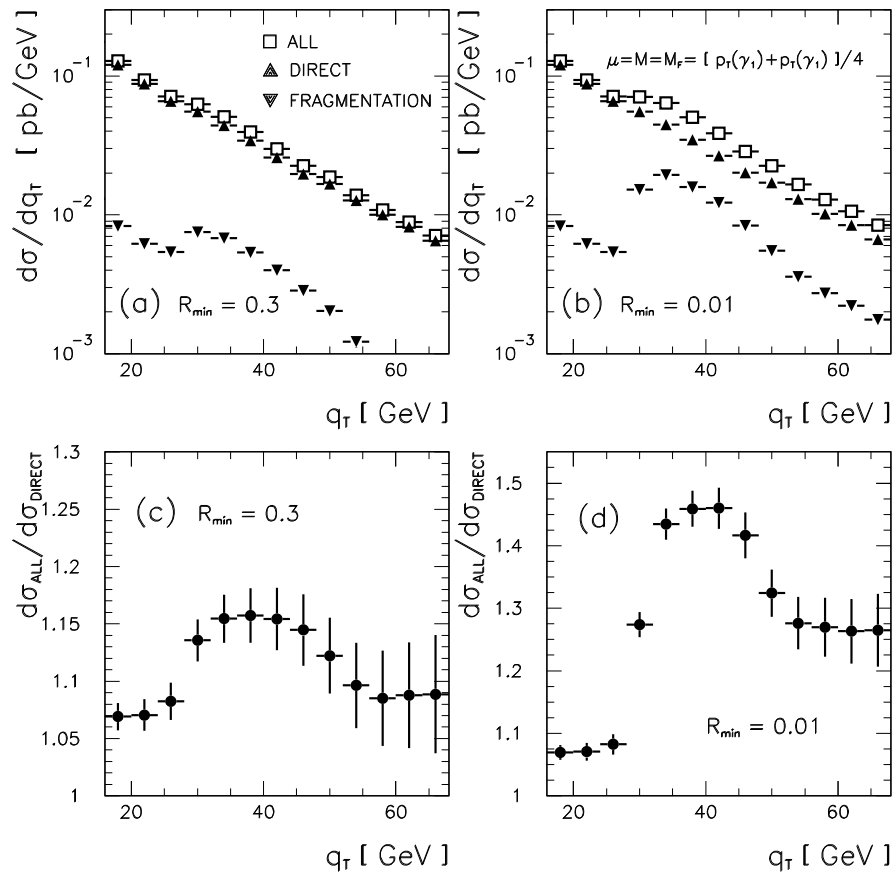


Figure 4: Top: the q_T spectrum (open squares) split into direct (full triangles) and fragmentation part (inverted triangles) for $R_{min} = 0.3$ (a) and $R_{min} = 0.01$ (b). Bottom: the ratio of the total q_T distribution divided by the direct one for $R_{min} = 0.3$ (c) and $R_{min} = 0.01$ (d).

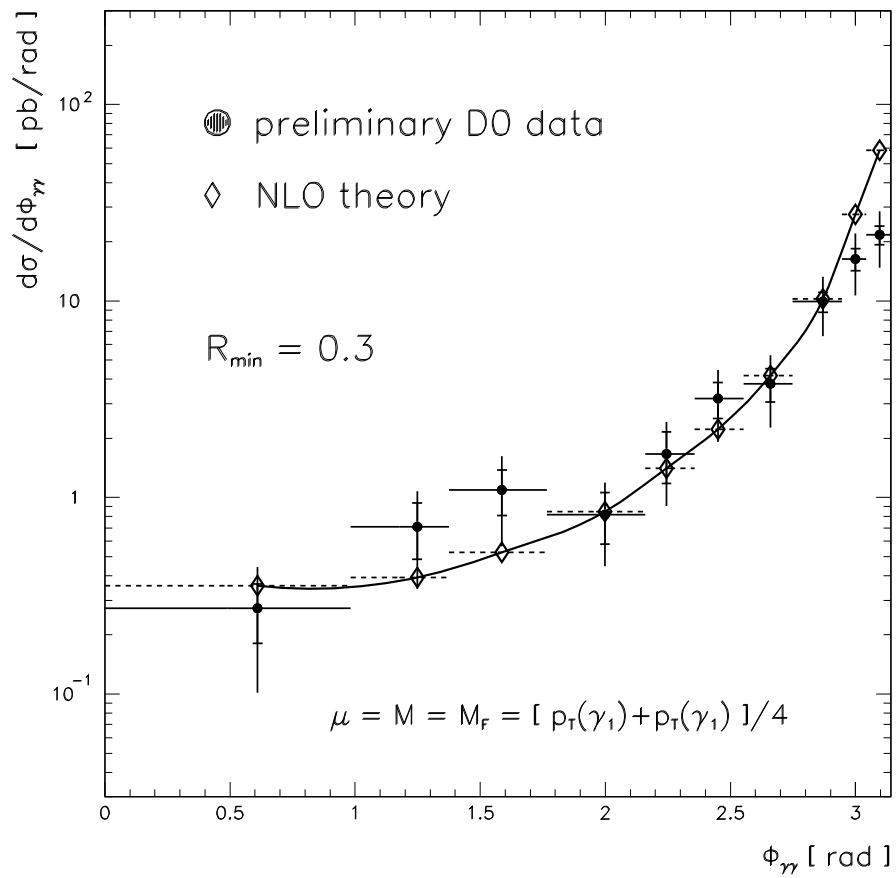


Figure 5: $\phi_{\gamma\gamma}$ distribution of photon pairs. Black dots: D0 data [6], white diamonds: average values of the NLO calculation (DIPHOX code) in the corresponding experimental bins. The curve is a spline interpolation between the theoretical average.

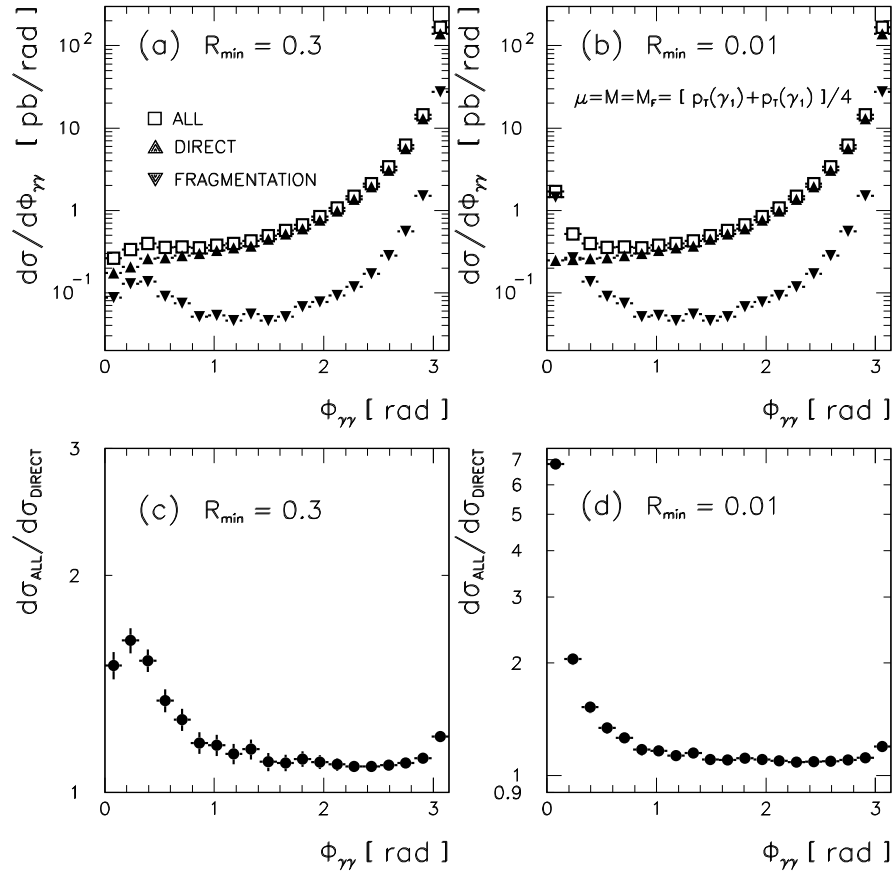


Figure 6: Top: the theoretical $\phi_{\gamma\gamma}$ distribution (open squares) split into direct (full triangles) and fragmentation part (inversed triangles) for $R_{\min} = 0.3$ (a) and $R_{\min} = 0.01$ (b). Bottom: the ratio of the total $\phi_{\gamma\gamma}$ distribution divided by the direct one for $R_{\min} = 0.3$ (c) and $R_{\min} = 0.01$ (d). The collinear enhancement of the fragmentation part for small $\phi_{\gamma\gamma}$ is clearly visible.